Fluorinated Amphiphilic Vinyl Ether Block Copolymers: Synthesis and Characteristics of Their Micelles in Water

Kozo Matsumoto, Hiroaki Mazaki, and Hideki Matsuoka*

Department of Polymer Chemistry, Kyoto University, Kyoto 615-8510, Japan

Received July 22, 2002; Revised Manuscript Received April 15, 2003

ABSTRACT: Fluorine-containing amphiphilic block copolymers, poly(2-hydroxyethyl vinyl ether)-*block*-poly(2-(2,2,2-trifluoroethoxy)ethyl vinyl ether)) (poly(HOVE-*b*-TFEOVE) (m = 78, n = 23)), poly(2-hydroxyethyl vinyl ether)-*block*-poly(2-(2,2,3,3,3-pentafluoropropoxy)ethyl vinyl ether) (poly(HOVE-*b*-PFPOVE) (m = 74, n = 22)), and poly(2-hydroxyethyl vinyl ether)-*block*-poly(2-(2,2,3,3,4,4,4-heptafluorobutoxy)ethyl vinyl ether) (poly(HOVE-*b*-HFBOVE) (m = 79, n = 19)) were synthesized along with the non-fluorine-containing amphiphilic block copolymer, poly(2-hydroxyethyl vinyl ether)-*block*-poly(*n*-butyl vinyl ether) (poly(HOVE-*b*-NBVE) (m = 70, n = 22)), where m and n are polymerization degrees of hydrophilic segment and hydrophobic segment, respectively. These fluorine-containing block copolymers considerably reduced the surface tension of the aqueous solutions, indicating the high surface activity of the block copolymers. They formed core−shell rodlike and/or core−shell spherical micelles in aqueous solutions, which were evaluated by small-angle neutron scattering (SANS), small-angle X-ray scattering (SAXS), and dynamic light scattering (DLS) analyses. A qualitative trend was observed, that is, the fraction of rodlike micelles increased, as the number of fluorine atoms in a hydrophobic segment increased. The fluorine-containing block copolymer selectively solubilized the hydrophobic fluorinated dye into water phase and the fluorinated dye selectivity increased as the number of the fluorine atoms in the hydrophobic monomer unit increased. Solubilization of a low molecular weight compound strongly affected the copolymer micelle structure, which was also confirmed by SANS, SAXS, and DLS analyses.

Introduction

Fluorinated polymers have attracted much attention because of their unique characteristics such as high hydrophobicity, lipophobicity, chemical stability, and biocompatibility.[1−3] The combination of fluorinated polymers with hydrophilic polymers may lead to a new class of polymeric amphiphiles.[4] Recent development of a living polymerization technique has enabled us to prepare various well-defined block copolymers containing fluorinated segments.[5−7] However, investigations of water-soluble fluorine-containing block copolymers have been limited so far.[8] In the previous study, we synthesized a water-soluble amphiphilic block copolymer, poly(2-hydroxyethyl vinyl ether)-*block*-poly(2-(2,2,2-trifluoroethoxy)ethyl vinyl ether), poly(HOVE-*b*-TFEOVE), which comprised a hydrophilic segment having the 2-hydroxyethyl groups and a hydrophobic segment having 2,2,2-trifluoroethoxy groups.[9] Although this polymer had only three fluorine atoms per one repeating unit in the hydrophobic segment, it exhibited peculiar properties such as high surface activity and "*fluorophilicity*" in the solubilization of fluorinated dyes in aqueous media. To understand more about this series of block copolymers, here we synthesized analogous vinyl ether block copolymers consisting of the same hydrophilic segments and various fluorinated hydrophobic segments, that is poly(TFEVOE-*b*-HOVE), poly(2-hydroxyethyl ether)-*block*-poly(2-(2,2,3,3,3-pentafluoropropoxy)ethyl vinyl ether) (poly(HOVE-*b*-PFPOVE)), and poly(2-hydroxyethyl vinyl ether)-*block*-poly(2-(2,2,3,3,4,-4,4-heptafluorobutoxy)ethyl vinyl ether) (poly(HOVE-*b*-HFBOVE)), by means of a living cationic polymerization.[10] Then we examined their surface activity, micelle structures, and solubilization properties toward hydrophobic compounds in aqueous media in comparison with the nonfluorinated amphiphilic vinyl ether block copolymer, poly(2-hydroxyethyl vinyl ether)-*block*-poly(*n*-butyl vinyl ether) (poly(HOVE-*b*-NBVE)).

We evaluated the surface activity and solubilization capability of the block copolymers by surface tension measurements of the aqueous solutions and UV adsorption spectroscopy of dye-solubilized block copolymer solutions, respectively. We also utilized small-angle neutron scattering (SANS), small-angle X-ray scattering (SAXS), and dynamic light scattering (DLS) analysis to elucidate the micelle structure and the effect of dye solubilization on the micelle structures in detail.

Experimental Section

Materials. 2-Hydroxylethyl vinyl ether (HOVE) was kindly donated by Professor Mitsuo Sawamoto of Kyoto University. 2-Vinyloxyethyl ethanesulfonate,[9a] 2-acetoxyethyl vinyl ether (AcOVE),[11] 2-(2,2,2-trifluoroethoxy)ethyl vinyl ether (TFEOVE),[9a] 2-(2,2,3,3,3-pentafluoropropoxy)ethyl vinyl ether (PFPOVE),[12] and *n*-butyl vinyl ether−HCl adduct[13] were prepared by the reported procedures. 2,2,3,3,4,4,4-Heptafluoro-1-butanol was purchased from Daikin (Tokyo, Japan). Sodium hydride (ca. 30 wt % in mineral oil), chlorobenzene, 1,4-dioxane, and sodium hydroxide were purchased from Wako Pure Chemical (Osaka, Japan); zinc chloride (1.0 M diethyl ether solution) was purchased from Aldrich (Milwaukee, WI) and used as delivered. *n*-Butyl vinyl ether (NBVE) was purchased form Wako and distilled twice over calcium hydride. Tetrahydrofuran (THF) and diethyl ether were freshly distilled over sodium benzophenone ketyl under an argon atmosphere, and methylene chloride was distilled over calcium hydride before use. D_2O (99.9% atom D) used for SANS experiments was purchased from Aldrich.

Synthesis of 2-(2,2,3,3,4,4,4-Heptafluorobutoxy)ethyl Vinyl Ether (HFBOVE). Sodium hydride (60 wt % oil suspension, 16 g, 390 mmol) was charged in a two-necked round-bottomed flask equipped with a magnetic stirring bar, reflux condenser, and septum rubber. The flask was flushed

* To whom correspondence should be addressed.

10.1021/ma021166i CCC: $27.50
Published on Web 02/17/2004

with nitrogen, and the sodium hydride was washed with dry hexane (50 mL) three times. Then the flask was filled with tetrahydrofuran (120 mL) and cooled to 0 °C. 2,2,3,3,4,4,4-Heptafluoro-1-butanol (50 g, 250 mmol) was slowly added, and vinyloxyethyl ethanesulfonate (44 g, 240 mmol) was then added. The mixture was stirred and heated under reflux for 24 h. Then the resulting mixture was poured into 1 M aqueous $NaHCO_3$ and extracted with diethyl ether. The organic layer was dried over anhydrous Na_2SO_4 and concentrated. The residual oil was distilled first over CaH_2 and then over NaH under reduced pressure to give the title compound (20 g, 73 mmol) in 31% yield; bp 69−70 °C (6.6×10^3 Pa). IR (neat): 2937, 2885, 1620, 1458, 1323, 1230, 1124, 1016, 964, 920 cm^{-1}. ^1H NMR δ ($CDCl_3$): 3.84−3.88 (m, 4H), 4.03 (t, $J_{H-F} = 14.8$ Hz, 2H), 4.06 (dd, $J = 2.2$, 6.3 Hz, 1H), 4.20 (dd, $J = 2.2$, 14.3 Hz, 1H), 6.48 (dd, $J = 6.3$, 14.3 Hz, 1H). ^{13}C NMR δ ($CDCl_3$): 67.21, 68.09 (t, $J_{C-F} = 26$ Hz), 7127, 87.02, 151.43. Anal. Calcd for $C_7H_9F_7O_2$: C, 35.57; H, 3.36%. Found: C, 35.61; H, 3.27%.

Block Copolymerization. Two Schlenk tubes equipped with a three-way stopcock were baked under nitrogen and used for the synthesis of each block copolymer. One (tube A) was for the synthesis of a homopolymer, and the other (tube B) was for the synthesis of a block copolymer. The reaction was initiated by sequential addition of a solution of *n*-butyl vinyl ether−HCl adduct (0.10 M in hexane, 2.5 mL, 0.25 mmol) and a solution of $ZnCl_2$ (0.1 M in diethyl ether, 0.80 mL, 0.08 mmol) into a mixture of AcOVE (1.90 mL, 15 mmol) and chlorobenzene (0.5 mL, as a GC internal standard) in methylene chloride (20 mL) at −20 °C. A small portion of reaction mixture in tube A (ca. 0.1 mL) was taken with a syringe and quenched with ammonia-containing methanol (1.5 wt %, 0.3 mL), which was analyzed by gas chromatography (Shimadzu GC-8A chromatograh equipped with glass column, stationary phase: silicon-DC11(20%), support: Celite 545S) to check the monomer conversion. After 95% of a monomer had been converted, the polymerization in tube A was terminated with ammonia-containing methanol (5 mL). On the other hand, tube B was cooled to −40 °C, and the second monomer (TFEOVE, PFPOVE, HFBOVE, or NBVE (5.0 mmol)) was added to the mixture. The polymerization in tube B was terminated with ammonia-containing methanol (5 mL) 4.0 h after the second monomer had been added. The resulting mixtures in tubes A and B were poured into water and the products were extracted with diethyl ether, respectively. The extracts were dried over Na_2SO_4 and concentrated in vacuo to give polyAcOVE homopolymer and the desired block copolymer (poly(AcOVE-*b*-TFEOVE), poly(AcOVE-*b*-PFPOVE), poly(AcOVE-*b*-HFBOVE), or poly(AcOVE-*b*-NBVE)).

Hydrolysis of Acetyl Protecting Group. The acetyl protecting groups of the block copolymers were hydrolyzed by treatment with an excess amount of aqueous sodium hydroxide (4.0 M, 5 equiv of NaOH to acetyl groups in 10 wt % polymer solution) in 1,4-dioxane for 3 days at room temperature. Removal of impurities by dialysis (Spectra/Pro 7, molecular weight cutoff 1000) in water for 1 week, followed by freeze-drying in vacuo gave poly(HOVE-*b*-TFEOVE), poly(HOVE-*b*-PFPOVE), poly(HOVE-*b*-HFBOVE), and poly(HOVE-*b*-NBVE).

Molecular Characterization. Gel permeation chromatography of the obtained polymers was carried out before hydrolysis in chloroform on a JASCO 880-PU chromatograph equipped with four polystyrene gel columns (Shodex K-802, K-803, K-804, and K-805) and JASCO 830-RI reflective index detector. In all cases, GPC charts clearly shifted to the high molecular weight region keeping narrow molecular weight distributions after addition of the second monomer, indicating the clean formation of the block copolymers. The values of M_w/M_n were determined by GPC with a polystyrene standard calibration for poly(AcOVE-*b*-TFEOVE), poly(AcOVE-*b*-PFPOVE), poly(AcOVE-*b*-HFBOVE), and poly(AcOVE-*b*-NBVE), where M_w and M_n are weight- and number-average molecular weights, respectively. Proton NMR spectra were recorded on a JEOL GSX 270 spectrometer, and those of poly(AcOVE-*b*-TFEOVE), poly(AcOVE-*b*-PFPOVE), poly(AcOVE-*b*-HFBOVE), and poly(AcOVE-*b*-NBVE) in $CDCl_3$ were similar to those of the analogous block copolymers reported previously.[9] The number-average degrees of polymerization of poly(AcOVE-*b*-TFEOVE), poly(AcOVE-*b*-PFPOVE), and poly(AcOVE-*b*-HFBOVE) were determined by comparing the area of acetoxy methyl peak (at 2.09 ppm) and methylene peak adjacent to the CF_2 group (at 3.75−3.93 ppm) with methyl peak (at 0.92 ppm) of the initiation end butyl group. Those of poly(AcOVE-*b*-NBVE) were determined as follows. First, the degree of polymerization for the AcOVE segment was determined by ^1H NMR measurement of the AcOVE homopolymer obtained from a termination of living polyAcOVE before adding NBVE. Then, the degree of polymerization for the NBVE segment was estimated from the integral ratio of acetoxy methyl peak of AcOVE segment at 2.09 ppm and methyl peak of NBVE segment at 0.92 ppm. Although the values were obtained for poly(AcOVE-*b*-TFEOVE), poly(AcOVE-*b*-PFPOVE), poly(AcOVE-*b*-HFBOVE), and poly(AcOVE-*b*-NBVE) precursor polymers, they can be applied for hydrolyzed polymers, poly(HOVE-*b*-TFEOVE), poly(HOVE-*b*-PFPOVE), poly(HOVE-*b*-HFBOVE), and poly(HOVE-*b*-NBVE) as well, since it was confirmed by ^1H NMR in D_2O that no subreaction had taken place during hydrolysis.

Surface Tension Measurements. The surface tension of an aqueous copolymer solution was measured on a CBVP-Z automatic surface tensiometer (Kyowa Interface Science Co., Ltd.) using a Pt plate in full automatic mode. The sample polymer solution (the concentration ranged from 10^{-6} to 3.2×10^{-3} mol/L) was prepared by direct dissolution of each polymer in ultrapure water obtained by a Millipore Milli-Q system, and the measurements were done at least 3 days after sample preparation.

Small-Angle Neutron Scattering (SANS). The SANS measurements were performed by SANS-U of Institute for Solid State Physics, The University of Tokyo, at the research reactor JRR-3, Tokai, Japan. The wavelength (λ) of neutron beam was 7 Å ($\Delta\lambda/\lambda = 10\%$). Polymer solutions ($3.2 \times 10^{-4}$ mol/L) were prepared by direct dissolution of the block copolymer into D_2O (an excess amount of powder solubilizate was added for solubilization sample) and filtrated through a membrane (Millex-GV, Millipore, pore size of 0.22 μm). Solutions were measured in quartz cells (Nippon Silica Glass Co., Tokyo) with a pass length of 4 mm at 25 °C 5 days after sample preparations. Scattering data measured by a 2D detector were circular averaged to 1D and then corrected for electronic background, and the scattering of the empty cell was subtracted. The data were transformed to absolute intensities using the Lupolen standard. From all scattering data of samples, we subtracted the scattering of solvent and the calculated incoherent scattering of the polymer. The SANS experiments were carried out at sample−detector distances of 1, 4, and 12 m, covering a range of the scattering vector (q) of $0.002 \le q \le 0.28$ $Å^{-1}$. The typical accumulation times of SANS runs were 1 h for 1 m sample−detector distance, 1 h for 4 m, and 3.5 h for 12 m.

Small-Angle X-ray Scattering (SAXS). The SAXS measurements were performed using a Kratky type camera (Rigaku Corp., Tokyo) equipped with a rotating anode X-ray generator and a 1D position-sensitive proportional counter (PSPC). The details of the apparatus and data treatment were as fully described elsewhere.[14] Polymer solutions (3.2 mmol/L) were prepared by directly dissolving the block copolymer into ultrapure water (an excess amount of solubilizate was added for solubilization sample) and filtrated through a membrane (Millex-GV, Millipore, pore size of 0.22 μm). Sample solutions were measured in glass capillaries (Mark, Berlin) with a diameter of 2 mm at 25 °C 5 days after sample preparation. The typical accumulation time of a SAXS run was about 3 h. In experimental data, the scattering from pure water was subtracted.

Data Analysis of SANS and SAXS Measurements. A similar basic principle can be applied for both SANS and SAXS analyses. The main difference is that the neutron is scattered by the density fluctuation of scattering length, while the scattering of X-ray occurs by the electron density fluctuation.

When the contribution of interparticle interaction is negligible, the scattering intensity $d\Sigma(q)/d\Omega$ from an isolated

particle is given by the equation

$$d\Sigma(q)/d\Omega = n_p P(q) \quad (1)$$

where n_p is the number density of particles and $P(q)$ is the particle form factor. The scattering vector q is defined by $q = 4\pi \sin \theta/\lambda$, where 2θ is the scattering angle and λ is the wavelength of neutron or X-ray. Here we deal with the micelles having a core−shell structure with the homogeneous electron density in the core and the shell regions. In such a model, the hydrophobic segment (ROVE) forms the core, and the shell contains hydrophilic segment (HOVE) hair and solvent water. The particle form factor of a core−shell model can be written as follows:

$$P(q) = (1/2)\int_0^{\pi}\{(\rho_C - \rho_S)V_C F_C(q) + (\rho_S - \rho_0)V_S F_S(q)\}^2 \sin\beta \, d\beta \quad (2)$$

where ρ_C, ρ_S, and ρ_0 are the scattering length densities (for SANS) and electron densities (for SAXS) of the core, the shell, and the solvent, respectively. V_C and V_S are the volumes of the core and the overall micelle, respectively. The scattering amplitude $F_i(q)$ (i = c or s, where c and s denote the core and the shell) depends on the size and shape of the scattering particles.

For a monodisperse isolated sphere with a radius of R_i, $F_i(q)$ is given by

$$F_i(q) = 3\{\sin(qR_i) - qR_i \cos(qR_i)\}/(qR_i)^3 \quad (3)$$

Using the value of the electron density of the monomer unit ρ_{ROVE} and ρ_{HOVE}, ρ_c and ρ_s can be represented by

$$\rho_c = \rho_{ROVE} \quad (4)$$

$$\rho_s = \phi_{sol}\rho_0 + (1 - \phi_{sol})\rho_{HOVE} \quad (5)$$

where ϕ_{sol} is the volume fraction of the solvent in the shell, which can be calculated by the following equation with the degree of polymerization of HOVE (m), the volume of HOVE repeating units (v_{HOVE}), the volume of the core (V_c), and the volume of the overall micelle (V_s):

$$\phi_{sol} = 1 - N_{agg} m v_{HOVE}/(V_s - V_c) \quad (6)$$

N_{agg} denotes the aggregation number of the micelles, which is calculated from V_c, the degree of polymerization of hydrophobic segment (n), and the volume of its repeating units (v_{ROVE}):

$$N_{agg} = V_c/(n v_{ROVE}) \quad (7)$$

Assuming that all polymers contribute to the micelle formation, the number density n_p of the micelles is calculated

$$n_p = \phi_{polym}/(N_{agg}(n v_{ROVE} + m v_{HOVE})) \quad (8)$$

where ϕ_{polym} is the volume fraction of copolymer in solution.

For a rodlike structure with a core radius of R_c, the overall micelle radius R_s, and rod length L, the scattering amplitude is given by

$$F_i(q) = \{(\sin(q(L_i/2)\cos\beta)/(q(L_i/2)\cos\beta)\}\{2J_1(qR_i \sin\beta)/(qR_i \sin\beta)\} \quad (9)$$

where β is the angle between the axis of symmetry of rod and the scattering vector q. J_1 denotes the Bessel function of the first order. If $q \gg 2\pi/L$ and $L \gg R_s$, the form factor of rodlike micelle can be reduced to

$$P(q) = (\pi/qL)\{(\rho_c - \rho_s)V_c 2J_1(qR_c)/(qR_c) + (\rho_s - \rho_0)V_s 2J_1(qR_s)/(qR_s)\}^2 \quad (10)$$

For SAXS data analysis, we introduced a shift factor f, since the intensity of the experimental data is obtained in arbitrary units because the values were not calibrated to an absolute scale. Therefore, the relative scattering intensity $I(q)$ is given by

$$I(q) = f\, n_p P(q) \quad (11)$$

The electron densities of $\rho_{TFEOVE} = 0.43$, $\rho_{PFPOVE} = 0.46$, $\rho_{HFBOVE} = 0.48$, $\rho_{NBVE} = 0.32$, $\rho_{HOVE} = 0.49$, and $\rho_0 = 0.33$ [Å^{-3}] and the scattering length density of $\rho_{TFEOVE} = 1.17 \times 10^{10}$, $\rho_{PFPOVE} = 1.93 \times 10^{10}$, $\rho_{HFBOVE} = 2.09 \times 10^{10}$, $\rho_{NBVE} = 4.69 \times 10^8$, $\rho_{HOVE} = 8.45 \times 10^9$, and $\rho_0 = 6.41 \times 10^{10}$ [cm^{-2}] were fixed. These values were calculated from the electron number or scattering length in each monomer unit, unit formula weight, and bulk density of each monomer and solvent. The bulk density of 1.39 g/cm^3 for polyTFEOVE, 1.50 g/cm^3 for polyPFPOVE, 1.58 g/cm^3 for polyHFBOVE, 0.95 g/cm^3 for polyNBVE, and 1.49 g/cm^3 for polyHOVE were used. In the core−shell model fitting, three parameters, R_c, R_s, and f were variable, while the value of f was arranged to be the same in each SAXS measurement sequence.

For the sphere−rod coexistence model, the scattering intensity is given by

$$d\Sigma(q)/d\Omega_{sphere-rod} = n_p\phi_{Nsphere}P(q)_{sphere} + n_p\phi_{Nrod}P(q)_{rod} \quad (12)$$

where $\phi_{Nsphere}$ and ϕ_{Nrod} are number fractions of the sphere and rodlike micelles in the total number of micelles in the solution; $P(q)_{sphere}$ and $P(q)_{rod}$ are form factors of the corresponding micelles. Equation 12 can be written as follows:

$$d\Sigma(q)/d\Omega_{sphere-rod} = (m_p\phi_{sphere}/N_{sphere})P(q)_{sphere} + (m_p\phi_{rod}/N_{rod})P(q)_{rod} \quad (13)$$

where m_p is the number density of polymer molecules, ϕ_{sphere} and ϕ_{rod} are volume fractions of the micelles in the total volume of micelles, and N_{sphere} and N_{rod} are the aggregation numbers of the sphere and disklike micelles.

Dynamic Light Scattering (DLS). The DLS measurements were performed on a dynamic light scattering apparatus of Brookhaven Instruments (Holtsville, NY) equipped with a goniometer (BI-30), the correlator (BI-9000), and an Ar laser Spectra Physics model 2020-05 (Mountain View, CA). The wavelength of 488 nm was chosen by prism assembly. Polymer solutions (3.2×10^{-4} mol/L) were prepared in the same way as described in SAXS measurements and put into a DLS cell tube. The measurements were performed at 25 °C 5 days after sample preparations. Typical measuring angles were 60°, 75°, 90°, and 105°. Single-exponential fitting, double-exponential fitting, and the CONTIN method were applied for the data analysis.

Solubilization Experiments. UV−vis spectra of dye-solubilized polymer solutions were taken on a U-3310 spectrophotometer (Hitachi, Ltd.) using the same concentration of the polymer solution as a reference. The dye-solubilized polymer solutions were prepared by adding an excess amount of a powdered dye (300 mg) to an aqueous solution of block copolymers (10 mL) and by stirring the mixture for at least 3 days at room temperature. In this study, the excess dyes were precipitated at the bottom of the sample containers, which indicated that the solutions were saturated with the dyes.

Results and Discussion

Synthesis of Amphiphilic Block Copolymers. We synthesized three fluorine-containing precursor block copolymers, poly(AcOVE-*b*-TFEOVE), poly(AcOVE-*b*-PFPOVE), and poly(AcOVE-*b*-HFBOVE), which have three, five, and seven fluorine atoms in one hydrophobic monomer unit, respectively, by sequential cationic polymerizations of acetyl protecting 2-hydroxyethyl vinyl ether (AcOVE) with corresponding vinyl ether

Scheme 1

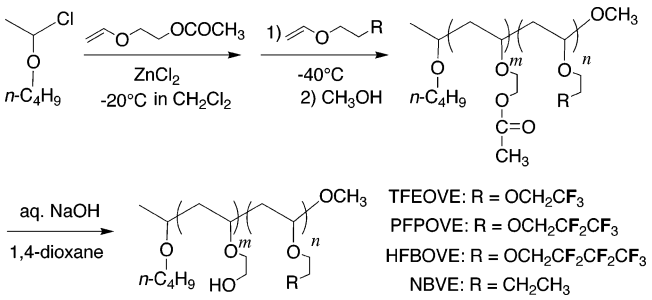

Table 1. Characteristics of the Amphiphilic Block Copolymers[a]

polymer	*m* ^{1}H NMR	*n* ^{1}H NMR	M_n ^{1}H NMR	M_w/M_n GPC
poly(HOVE-*b*-TFEOVE)	78	23	10 900	1.12
poly((HOVE-*b*-PFPOVE)	74	22	11 500	1.10
poly(HOVE-*b*-HFBOVE)	79	19	12 200	1.09
poly(HOVE-*b*-NBVE)	70	22	8 900	1.17

[a] *m* = number-average polymerization degree of hydrophilic segment, and *n* = number-average polymerization degree of hydrophobic segment.

monomers (Scheme 1). The semifluorinated monomers involved here are very useful because the electron-withdrawing fluoroalkyl groups are introduced far away from vinyl groups so that the substituents do not affect the reactivity of the active center in the polymerization. In addition, the monomers and their homopolymers are completely soluble in dichloromethane even at −40 °C. For comparison, we also prepared one non-fluorine-containing block copolymer poly(AcOVE-*b*-NBVE) by the same method. Gel permeation chromatograms of the obtained copolymers using chloroform as an eluent were monomodal with narrow molecular weight distributions (1.09−1.17) and observed in a higher molecular weight region than the AcOVE homopolymer, indicating a clean formation of block copolymers. The polydispersitiy for the homoAcOVE prepolymer were in the range 1.07−1.09, which indicated both hydrophobic and hydrophilic segments of the block copolymers had sufficiently narrow polydispersities. The polymerization degree of each segment was determined by ^{1}H NMR analysis of the end groups of the polymer. These copolymers were treated with sodium hydroxide in 1,4-dioxane to hydrolyze acetyl-protecting groups of polyAcOVE segment as shown in Scheme 1. The copolymers thus synthesized were purified by dialysis against water and freeze-dried to obtain powder samples. The molecular characteristics of the samples are listed in Table 1. All samples had approximately the same chain lengths in hydrophilic segments (HOVE) and in hydrophobic segments (TFEOVE, PFPOVE, HFBOVE, and NBVE). These block copolymers were directly soluble in both water and nonpolar organic solvents such as chloroform, confirming the amphiphilic character of the block copolymers. Using these samples, one can compare the effect of the pendant groups in the hydrophobic segments in aqueous media.

Surface Activity of the Block Copolymers. To examine the surface activities of the block copolymers in aqueous media, we measured the surface tension of the water solutions. Figure 1 shows the surface tensions of aqueous block copolymer solutions as a function of copolymer concentration. The surface tensions declined with increasing polymer concentration in all cases,

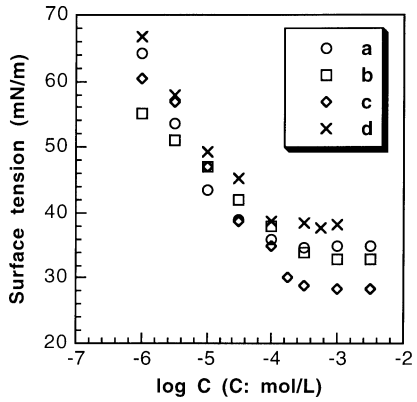

Figure 1. Surface tension of the aqueous solutions of amphiphilic block copolymers for (a) poly(HOVE-*b*-TFEOVE), (b) poly(HOVE-*b*-PFPOVE), (c) poly(HOVE-*b*-HFBOVE), and (d) poly(HOVE-*b*-NBVE) as a function of copolymer concentrations.

indicating that the block copolymer was adsorbed at the water surface. The breakpoint of the declining surface tension was observed at around 1.0×10^{-4} mol/L, where the critical micelle concentration (cmc) of the block copolymers may exist. The surface tension of the block copolymers above the cmcs decreased as the number of fluorine atoms per monomer unit increased. Particularly, the surface tension of poly(HOVE-*b*-HFBOVE) solution dropped to 28 mN/m. These results imply the high surface activity of the fluorine-containing block copolymers.

Structure of the Block Copolymer Micelle in Water. By using SANS, SAXS, and DLS techniques, we examined the structure of these associating copolymers in water. Figure 2 shows the SANS profiles for 3.2×10^{-4} mol/L copolymer solutions in D_2O. A strong scattering was observed in small-angle regions, indicating the existence of polymer assemblies. A clear q^{-1} dependence of scattering intensity was observed in the profiles (b), (c), and (d), which suggested the formation of rodlike micelles. On the other hand, profile (a) showed much gentler slope, which indicated a possibility of coexistence of rodlike and spherical micelles. We have already reported coexistence system of rodlike and spherical micelles about an amphiphilic poly(vinyl ether).[15] Figure 3 represents the SAXS profiles of the copolymer solutions measured under the same conditions as SANS experiments. Instead of D_2O, H_2O was used as a solvent for SAXS measurements. The micelle formations by the block copolymers were also supported by a strong X-ray scattering in the small-angle regions. In these cases, a clear second maximum of the scattering due to an intraparticle structure such as core−shell structure was observed around $q = 0.04-0.08$ Å^{-1}. We also carried out SAXS measurements of these samples at polymer concentration of 1.0×10^{-3} mol/L, and the profiles normalized by polymer concentrations were completely the same as obtained at 3.2×10^{-4} mol/L. It suggested that the micelle structures were kept unchanged at leased in these dilute concentrations. To analyze these scattering data in detail, we assumed both core−shell rodlike micelle and core−shell spherical micelle models and calculated the theoretical profiles for SANS and SAXS. The model micelle composed of core with bulk density of a core-forming polymer segment[16] and shell with constant density of shell-forming polymer segment swollen by solvent. The radii of the core (R_c) or the radii of the whole micelle (R_s) in the cross section of a

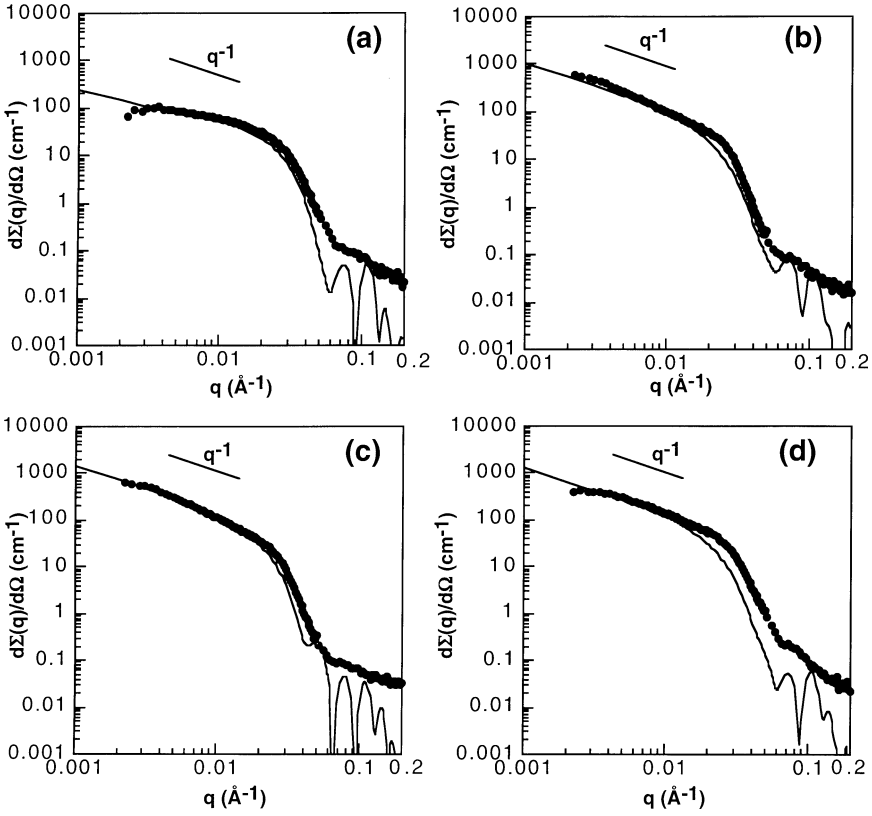

Figure 2. SANS profiles for 3.2×10^{-4} mol/L D_2O solutions of (a) poly(HOVE-*b*-TFEOVE), (b) poly(HOVE-*b*-PFPOVE), (c) poly(HOVE-*b*-HFBOVE), and (d) poly(HOVE-*b*-NBVE). Solid lines are the best fitted curves calculated from core−shell micelle models.

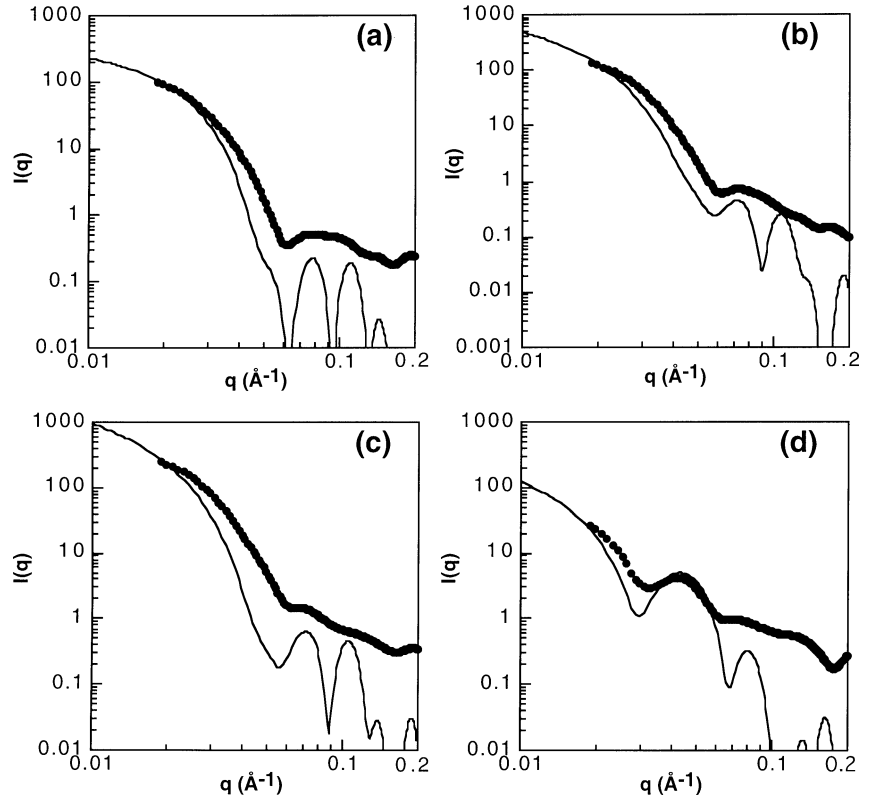

Figure 3. SAXS profiles for 3.2×10^{-4} mol/L aqueous solutions of (a) poly(HOVE-*b*-TFEOVE), (b) poly(HOVE-*b*-PFPOVE), (c) poly(HOVE-*b*-HFBOVE), and (d) poly(HOVE-*b*-NBVE). Solid lines are the best fitted curves calculated from core−shell micelle models.

spherical micelle and a rodlike micelle were assumed to be the same in the models, and the R_s and R_c have no size distribution. Naturally the following facts should be noted. (1) The cross-section radii of spherical and rodlike micelle should be different to some extent. (2) The core density differs from the bulk density of the

Table 2. Structural Parameters of the Block Copolymer Micelles[a]

				sphere			rod		
polymer	ϕ_{rod}	R_c [Å]	R_s [Å]	N_{agg}	ϕ_{sol}	R_h [Å]	N_{agg}/L	ϕ_{sol}	R_h [Å]
poly(HOVE-*b*-TFEOVE)	0.1	55	110	130	0.79	100	1.9	0.51	500
poly(HOVE-*b*-PFPOVE)	0.7	53	110	120	0.83	100	1.6	0.60	600
poly(HOVE-*b*-HFBOVE)	0.8	55	110	130	0.74	150	1.7	0.53	1100
poly(HOVE-*b*-NBVE)	0.4	55	120	180	0.79	120	2.4	0.50	550

[a] ϕ_{rod} = volume fraction of the rodlike micelle, R_c = sectional radius of the micelle core, R_s = sectional radius of the overall micelle, Φ_{sol} = volume fraction of the solvent in the shell, R_h = hydrodynamic radius of the micelle, L = length of the rodlike micelle [Å], and N_{agg} = aggregation number.

core-forming segment. (3) The shell density is not constant but radially changes. (4) The micelle core and shell have their own size distributions. However, to reduce the fitting parameters and discuss the results as simple as possible, we applied a rather strict micelle model here. The solid lines shown in Figures 2 and 3 were the fitting curves and they almost reproduced both of SAXS and SANS experimental data with the same fitting parameters in all cases. The deviation at larger angles is due to the fact that the scattering at larger angles is dominated by individual fluctuation of polymer chains in the shell (blob scattering),[17,18] which was not considered in the present model. Recently, Pedersen et al. proposed a new scattering theory for polymer micelle taking the influence of blob scattering into account.[19] An analysis by this new theory might bring us more detailed information on the structure of corona. The smearing of the scattering minimum at $q \sim 0.05$ Å^{-1} for SANS and at 0.06 Å^{-1} for SAXS was due to the polydispersity of the micelle size.[20] The fitting parameters are listed in Table 2. Poly(HOVE-*b*-TFEOVE) predominantly formed spherical micelles, while poly(HOVE-*b*-PFPOVE) and poly(HOVE-*b*-HFBOVE) mainly formed rodlike micelles. Poly(HOVE-*b*-NBVE) formed both rodlike micelles and spherical micelles in the comparable volume fractions. We noticed that rodlike micelles were more likely to be formed in a highly fluorinated block copolymer solutions, while the cross-sectional micellar size (R_c or R_s) were almost unchanged regardless of the number of fluorine atoms per monomer unit. The Guinier region of the rodlike micelles could not be observed in the experimental q range, and the averaged length of the rodlike micelles were considered to be quite large (>2000 Å).

One may have a strange feeling for the core size thus estimated since it is comparable for the contour length of hydrophobic chain. This means that the hydrophobic chains are almost fully stretched. However, the similar observations were reported also by other groups. Montensen et al. found the core radius (R_c) of 56 Å for the polystyrene ($PS_{9.6}$)-*b*-poly(ethylene oxide) ($PEO_{68.2}$) micelle.[21] Also, Jada et al. reported $R_c = 31$ Å for the PS_{10}-*b*-PEO_{50} micelle.[22] These radius are almost comparable to the contour length of hydrophobic chains. On the other hand, for PEO−PPO (poly(propylene oxide))−PEO micelle systems, rather small core formation was reported: Glatter et al. estimated $R_c = 25-30$ Å for $PEO_{27}-PPO_{39}-PEO_{27}$,[23] Mortensen et al.[24] reported $R_c = 40-50$ Å for $PEO_{25}-PPO_{40}-PEO_{25}$, and $R_c = 30$Å was found for $PEO_{13}-PPO_{30}-PEO_{13}$ by Wu et al.[25] The difference between these two systems is though to be due to the bulkiness of the side chain groups. PPO has small side groups, so it can form very compact micelle core. However, PS has a large side group, i.e., phenyl ring, the core becomes large, and its radius apparently looks to be comparable to the chain length. Nakano et al. studied poly(hydroxyethyl vinyl ether) (HOVE)-*b*-poly(*n*-butyl vinyl ether) (NBVE) micelles in aqueous solution and found the situation just in between two extreme cases mentioned above. NBVE has a side group which is larger than that of PPO but smaller than that of PS. Hence, the larger the partial molar volume of the side group of the hydrophobic chain, the larger the micelle core, even when the contour length of the chains are equivalent. Nakano et al. also reported that hydrophobic chains in the core are more stretched when its chain length is shorter. In the present case here, fluorinated hydrophobic chains have rather large side groups, but not so large as the phenyl group, and the degree of polymerization is also not so high (19−23); the comparable R_c values with hydrophobic chain length are reasonable and justified.

DLS results of the copolymer micelle solutions are consistent with the above considerations. Figure 4 shows the hydrodynamic size distributions of block copolymer micelles in water obtained from CONTIN analysis of the data at 90°. Bimodal size distributions were produced with all samples. Particles of hydrodynamic radius (R_h) from 100 to 200 Å can be considered as spherical micelles and those of 500 Å or larger R_h as rodlike micelles. It was also confirmed that poly(HOVE-*b*-TFEOVE) mainly formed spherical micelles and poly(HOVE-*b*-PFPOVE) and poly(HOVE-*b*-HFBOVE) mainly formed rodlike micelles, while poly(HOVE-*b*-NBVE) formed both spherical and rodlike micelles. We analyzed the DLS data at different scattering angles (60°, 75°, 90°, and 105°) by double-exponential fitting. All time correlation functions could be reproduced by adopting two decay rates Γ_1 and Γ_2 and the amplitudes A_1 and A_2. The typical time correlation functions and their fitting curves are depicted in Figure 5. The Γ/q^2 values were plotted against q^2 as shown in Figure 6. Almost constant values of Γ/q^2 were obtained in all q^2 range, which indicated that these dynamic modes were translational motion. The translational diffusion coefficients (D) were evaluated from the slope of the straight line using the relation of $\Gamma = Dq^2$. The R_h values were calculated from the diffusion coefficients using the Stokes−Einstein relation $R_h = k_B T/(6\pi\eta_0 D)$, where k_B, T, and η_0 represent Boltzmann constant, absolute temperature, and solvent viscosity, respectively. The estimated R_h values for the block copolymer micelles are listed in Table 2.

It is obvious the coexistence of spherical and rodlike micelles in the present system by the self-consistence results by SANS, SAXS, and DLS above. However, it is often claimed the possibility of an ellipsoidal micelle formation instead of sphere/rod coexistence when SAXS and/or SANS fitting is not perfect, ignoring the fact that this is a "model" fitting procedure. However, the ellipsoidal micelle formation is highly unrealistic by the concept of "packing parameter" proposed by Israela-

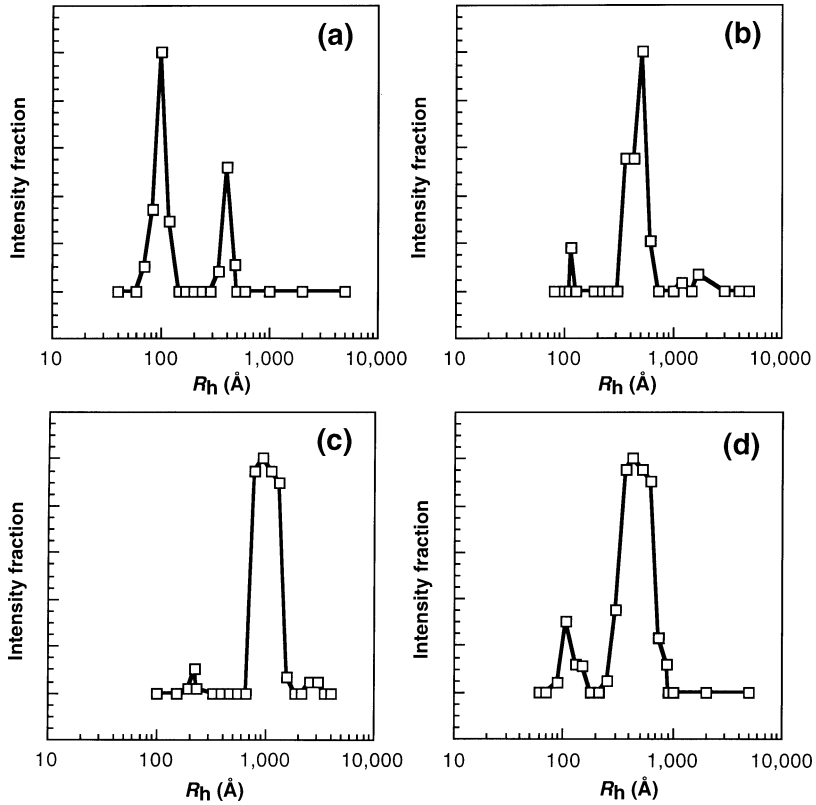

Figure 4. Micelle size distributions obtained from DSL CONTIN analysis for (a) poly(HOVE-*b*-TFEOVE), (b) poly(HOVE-*b*-PFPOVE), (c) poly(HOVE-*b*-HFBOVE), and (d) poly(HOVE-*b*-NBVE). R_h = hydrodynamic radius; scattering angle $\theta = 90°$.

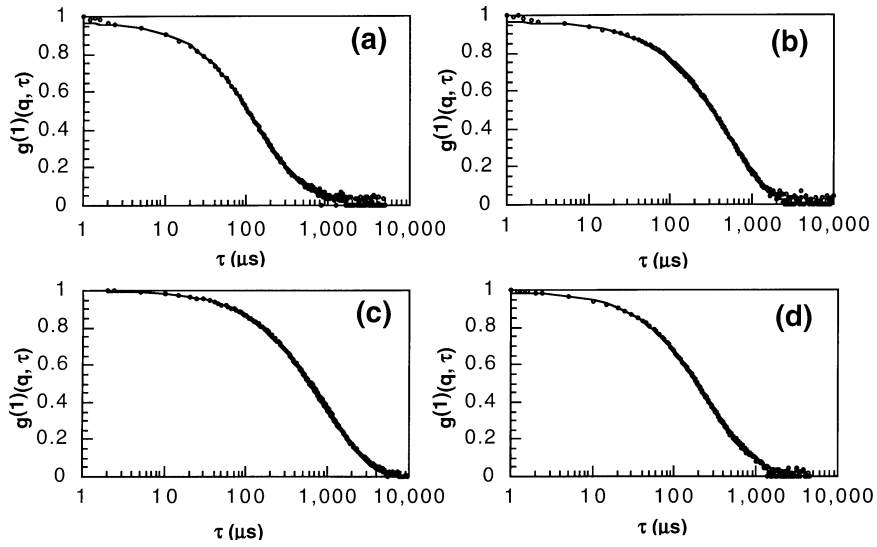

Figure 5. Time correlation functions for 3.2×10^{-4} mol/L aqueous solutions of (a) poly(HOVE-*b*-TFEOVE), (b) poly(HOVE-*b*-PFPOVE), (c) poly(HOVE-*b*-HFBOVE), and (d) poly(HOVE-*b*-NBVE) by DLS. Scattering angle $\theta = 90°$. Solid lines are the fitting curves obtained by double-exponential fitting. (a) $\Gamma_1 = 8700\ s^{-1}$, $\Gamma_2 = 1700\ s^{-1}$, $A_1 = 0.75$, $A_2 = 0.25$; (b) $\Gamma_1 = 8700\ s^{-1}$, $\Gamma_2 = 1500\ s^{-1}$, $A_1 = 0.20$, $A_2 = 0.80$; (c) $\Gamma_1 = 5800\ s^{-1}$, $\Gamma_2 = 790\ s^{-1}$, $A_1 = 0.18$, $A_2 = 0.82$; (d) $\Gamma_1 = 7300\ s^{-1}$, $\Gamma_2 = 1600\ s^{-1}$, $A_1 = 0.50$, $A_2 = 0.50$, where Γ_i is the decay rate and A_i is the amplitude for each mode.

chivili;[26] for the ellipsoidal shape, many kinds of amphiphilic molecules, which have a different parameter values, are necessary. In fact, for low molecular weight surfactant systems, a coexistence of sphere/rod micelles was confirmed and established, and this is now the common sense in conventional surfactant systems. Nonionic surfactants form spherical micelles at low temperature, but rodlike micelles forms above the critical temperature, and spherical and rod micelles are in dynamic equilibrium.[27] Also for the ionic surfactants, a similar phenomenon occurs above the critical salt concentration.[28] From these points of view, the finding of sphere/rod coexistence for polymer micelle system is significant and interesting. It might be highly valuable to find the critical condition for polymer micelle systems by changing physicochemical conditions, which should be our further target.

Recently, an atomic force microscope (AFM) technique was established very rapidly, and now it is almost a common technique to observe self-assemble systems. If we can observe micellar shape itself directly by AFM or TEM (transmission electron microscope), the situa-

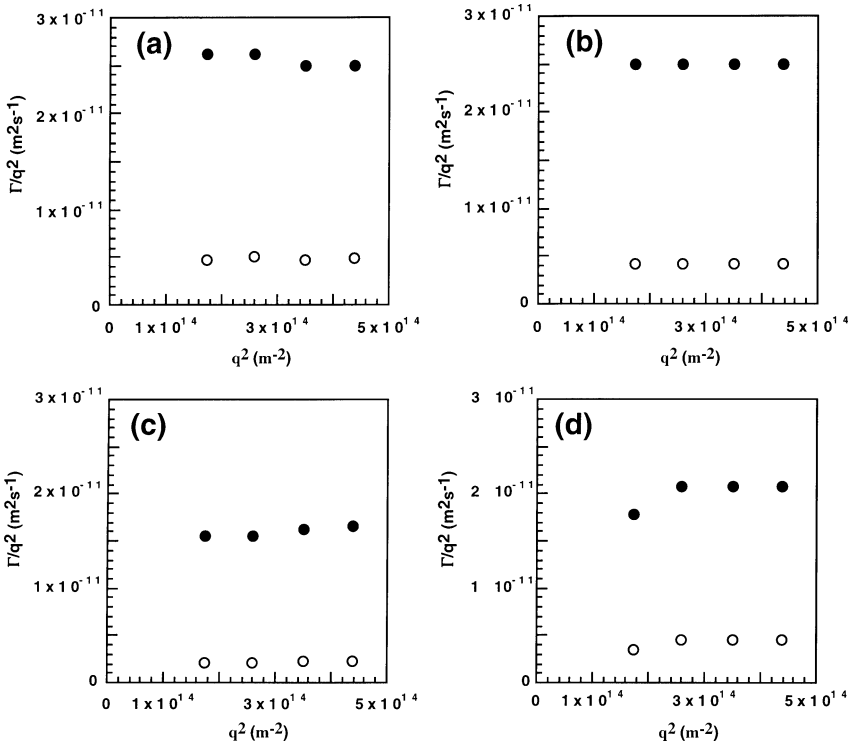

Figure 6. Γ/q^2 vs q^2 plot ((●) fast mode and (○) slow mode) for (a) poly(HOVE-*b*-TFEOVE), (b) poly(HOVE-*b*-PFPOVE), (c) poly(HOVE-*b*-HFBOVE), and (d) poly(HOVE)-*b*-NBVE.

tion in our system becomes clearer. In fact, we tried to look the micelle in this study, but it was unsuccessful. We could not observe micelle particles in AFM images. This is because polymer micelles were broken in the sample preparation process for AFM measurement. We tried a freeze-dry technique to prepare sample instead of simple drying, but the results were the same. The collapse of micelle "particle" is due to the low glass transition temperature (T_g) of hydrophobic chains forming a micelle core. The micelles which have a high-T_g core, such as polystyrene (T_g = 98 °C), can be easily observed by AFM.[29] Hence, it is highly difficult to observe micelle particles directly by commonly used techniques.

Solubilization of Hydrophobic Compound. Among many interesting properties of amphiphilic block copolymers, solubilization of small hydrophobic molecules into water could be the most attracting property from both academic and industrial points of view. Here, we examined the selective solubilization of certain hydrophobic compounds by using our fluorine-containing amphiphilic block copolymers. A mixture of fluorinated and nonfluorinated dyes was added to the block copolymer micelle solution, and the amount of solubilized dye was evaluated by UV absorption spectroscopy. Figure 7i shows the UV spectra of block copolymer aqueous solutions in the presence of decafluorobiphenyl (DFB) and 2,6-dimethylnaphthalene (DMN). Spectra of DFB (0.10 mmol/L) and DMN (0.10 mmol/L) in *n*-octane were also measured and depicted in the same figure. A clear increase of absorption around 265 nm, which is mainly caused by DFB, was observed as the number of fluorine atoms per monomer unit increased, while the absorption at 285 nm, which is mainly due to DMN, remained almost unchanged. Figure 7ii shows the spectra of copolymer solutions in the presence of DFB and *trans*-stilbene (Sti) along with spectra of DFB (0.10 mmol/L) and Sti (0.010 mmol/L) in *n*-octane. The absorption by

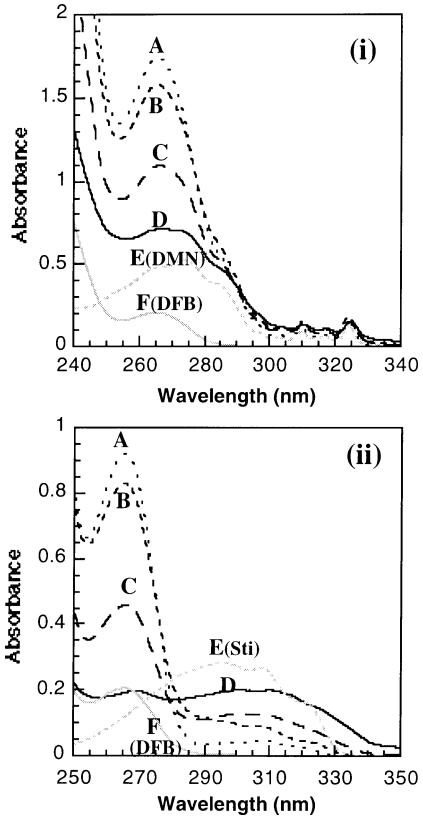

Figure 7. UV absorption spectra of block copolymer solutions (i) in the presence of DFB and DMN and (ii) in the presence of DFB and Sti: (A) poly(HOVE-*b*-HFBOVE), (B) poly(HOVE-*b*-PFPOBE), (C) poly(HOVE-*b*-TFEOVE), (D) poly(HOVE-*b*-NBVE), (E) 0.10 mmol/L DMN or 0.010 mmol/L Sti in *n*-octane, and (F) 0.10 mmol/L DFB in *n*-octane.

DFB at 265 nm increased, while the absorption by Sti at 300 nm decreased as the number of fluorine atoms

Table 3. Dye Concentrations (in μmol/L) Solubilized in the Amphiphilic Block Copolymer Solutions

	DFB + DMN		DFB + AN		DFB + Sti		OFN + AN	
	DFB	DMN	DFB	AN	DFB	Sti	OFN	AN
poly(HOVE-*b*-NBVE)	56	130	110	6.5	53	7.3	180	1.5
poly(HOVE-*b*-TFEOVE)	230	130	280	7.7	200	4.5	350	1.4
poly(HOVE-*b*-PFPOVE)	430	150	410	5.0	390	3.1	550	1.7
poly(HOVE-*b*-HFBOVE)	560	130	480	6.0	440	1.4	620	2.0

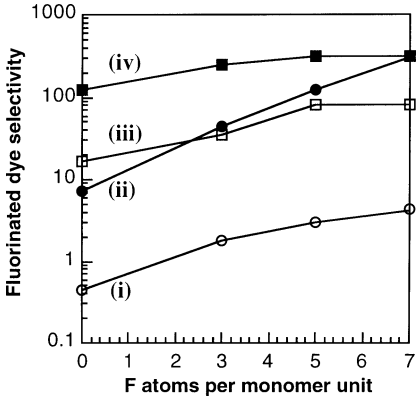

Figure 8. Fluorinated dye selectivity as a function of number of fluorine atoms per hydrophobic monomer unit for a mixture of (i) DFB and DMN, (ii) DFB and Sti, (iii) DFB and AN, and (iv) OFN and AN.

per monomer unit increased. Other combinations of fluorinated and nonfluorinated dyes, DFB and antracene (AN), or octafluoronaphthalene (OFN) and AN were also examined. The concentration of each dye solubilized by the block copolymers was evaluated by resolving the spectra into individual ones measured in *n*-octane. Table 3 summarizes the dye concentrations solubilized by the block copolymer micelles. The fluorinated dye selectivity ([fluorinated dye]/[nonfluorinated dye]) was plotted as a function of number of fluorine atoms per hydrophobic monomer unit in Figure 8. Fluorine-containing block copolymers are more likely to solubilize fluorinated dyes than non-fluorine-containing block copolymers, and the fluorinated dye selectivity was significantly enhanced by the increase of the fluorine atoms per monomer unit. From these results, we conclude that the fluorine-containing block copolymer has "fluorophilic" character.

Influence of Solubilization on the Micelle Structure. To examine the effect of solubilization of hydrophobic dyes on the micelle structures, SANS, SAXS, and DLS of poly(HOVE-*b*-TFEOVE), poly(HOVE-*b*-HFBOVE), and poly(HOVE-*b*-NBVE) solutions were taken after adding DFB. The SANS profiles are shown in Figures 9. Although difference of scattering length density in the micelle core by solubilization of DFB was negligible, the intensity of neutron scattering decreased practically by the solubilization in all SANS measurements. Figure 10 represents SAXS profiles of the copolymer solutions before and after adding DFB. The first slope of the SAXS profiles in the small-angle region became gentler, and the second maximum caused by micelle internal structure shifted to a larger angle region after adding DFB in all cases. These observations indicated that the micelles became smaller by solubilization. Interestingly, the SANS profiles of poly(HOVE-*b*-HFBOVE) and poly(HOVE-*b*-NBVE) still showed the q^{-1} dependence in the medium-angle region, while that of poly(HOVE-*b*-TFEOVE) showed a scattering pattern typical of a spherical micelle. We again analyzed the SANS and SAXS data by using the core−shell sphere and core−shell rodlike micelle model. Both SANS and

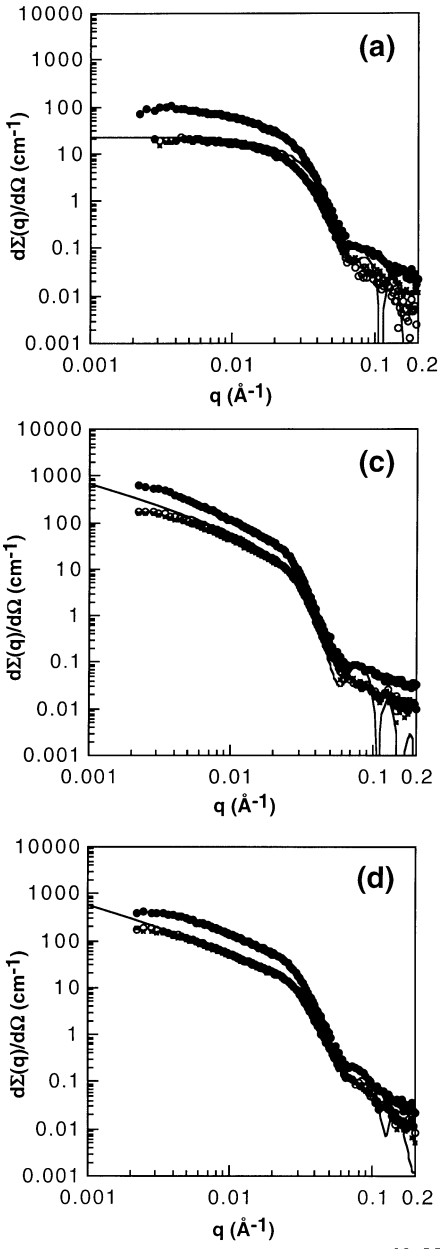

Figure 9. Comparison of SANS profiles obtained from the block copolymer solutions (●) with no dye, (○) with DFB, and (×) with DMN. Solid lines are the fitted curves for SANS data with a solubilizate. (a) poly(HOVE-*b*-TFEOVE), (c) poly(HOVE-*b*-HFBOVE), and (d) poly(HOVE-*b*-NBVE).

SAXS experimental data could be moderately reproduced by the same fitting parameters. The fitting parameters are listed in Table 4. Using DMN instead of DFB as a solubilizate, we examined SANS and SAXS of the block copolymer solutions. SANS and SAXS profiles of the block copolymer micelles solubilizing DMN gave almost same scattering curves as in the cases of DFB. As examples, SANS profiles for the block copolymer solutions with DMN are depicted in Figure 9.

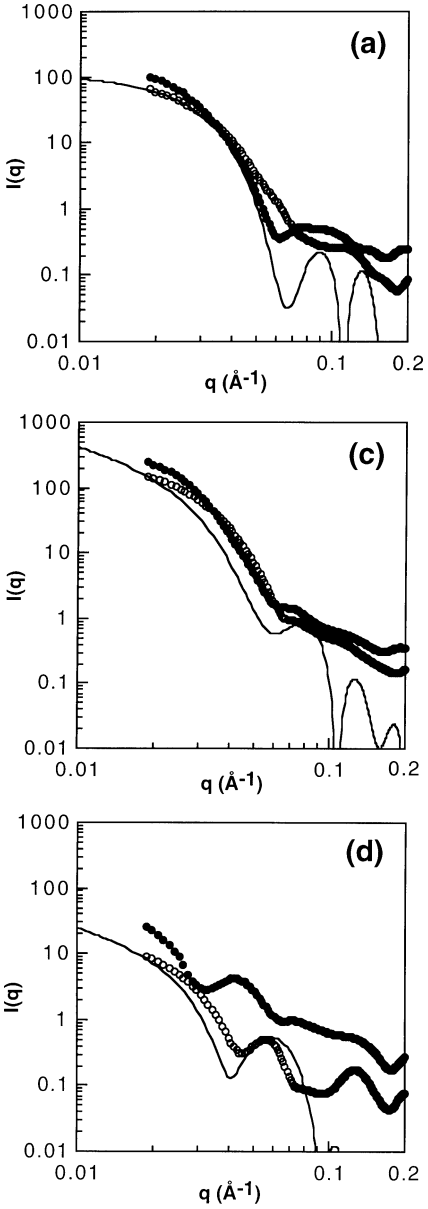

Figure 10. Comparison of SAXS profiles obtained from the block copolymer solutions (●) with no dye and (○) with DFB. Solid lines are the fitted curves for SAXS data with a solubilizate. (a) poly(HOVE-*b*-TFEOVE), (c) poly(HOVE-*b*-HFBOVE), and (d) poly(HOVE-*b*-NBVE).

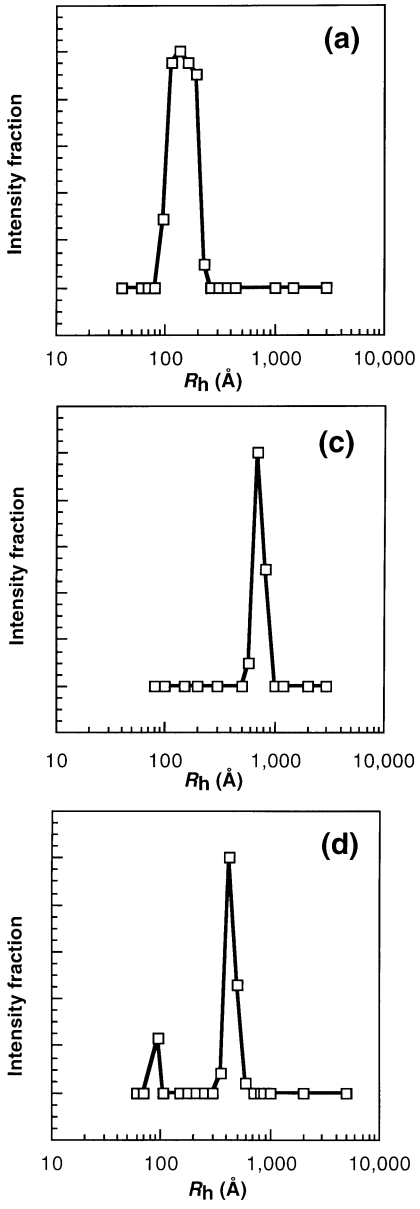

Figure 11. Micelle size distributions of the block copolymer solutions in the presence of DFB obtained from DSL CONTIN analysis (a) poly(HOVE-*b*-TFEOVE), (c) poly(HOVE-*b*-HFBOVE), and (d) poly(HOVE-*b*-NBVE). Scattering angle $\theta = 90°$.

Figure 11 shows the size distributions of the micelles analyzed by DLS after adding DFB. Poly(HOVE-*b*-TFEOVE) formed micelles with a hydrodynamic radius of ca. 100 Å, while poly(HOVE-*b*-HFBOVE) formed those of ca. 700 Å. Poly(HOVE-*b*-NBVE) formed micelles with hydrodynamic radii of ca. 100 and ca. 500 Å. The DLS data were further analyzed by single- or double-exponential fitting. Time correlation functions of the solutions obtained at scattering angle of 90° are given in Figure 12. The time correlation functions of poly(HOVE-*b*-TFEOVE) and poly(HOVE-*b*-HFBOVE) can be roughly reproduced by single-exponential fitting, while that of poly(HOVE-*b*-NBVE) is reproduced rather by double-exponential fitting. The Γ/q^2 values were plotted against q^2 in Figure 13. All modes show constant Γ/q^2 values, indicating that they are translational motions.

SANS, SAXS, and DLS analysis suggested that after solubilization of hydrophobic compounds the poly(HOVE-

Table 4. Structural Parameter of the Block Copoymer Micelles Solubilizing DFB[a]

				sphere			rod		
polymer	ϕ_{rod}	R_c [Å]	R_s [Å]	N_{agg}	ϕ_{sol}	R_h [Å]	N_{agg}/L	ϕ_{sol}	R_h [Å]
poly(HOVE-*b*-TFEOVE)	0	43	94	71	0.83	130			
poly(HOVE-*b*-HFBOVE)	1	35	95				0.70	0.78	720
poly(HOVE-*b*-NBVE)	0.5	35	84	47	0.86	100	0.99	0.63	520

[a] ϕ_{rod} = volume fraction of the rodlike micelle, R_c = sectional radius of the micelle core, R_s = sectional radius of the overall micelle, N_{agg} = aggregation number, Φ_{sol} = volume fraction of the solvent in the shell, R_h = hydrodynamic radius of the micelle, and L = length of the rodlike micelle [Å].

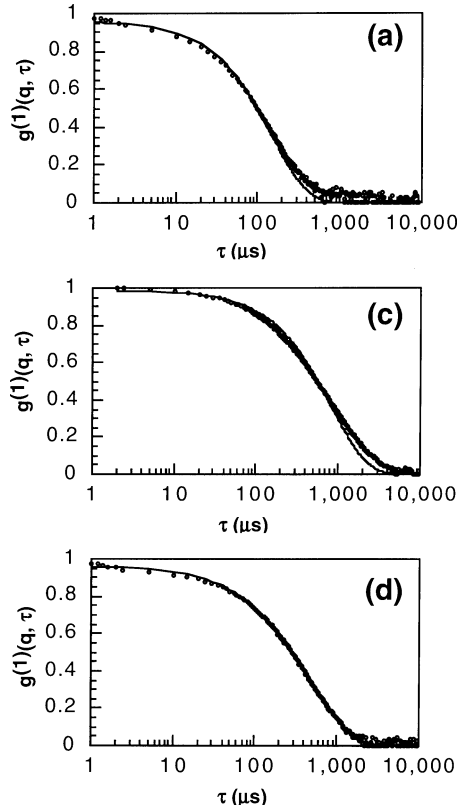

Figure 12. Time correlation functions for 3.2×10^{-4} mol/L aqueous solutions of (a) poly(HOVE-*b*-TFEOVE), (c) poly(HOVE-*b*-HFBOVE), and (d) poly(HOVE-*b*-NBVE) solubilizing DFB by DLS. Scattering angle $\theta = 90°$. Solid lines are the fitting curves obtained by single (a and c) or double (d) exponential fitting. (a) $\Gamma = 6700\ s^{-1}$, (c) $\Gamma = 1200\ s^{-1}$, and (d) $\Gamma_1 = 8700\ s^{-1}$, $\Gamma_2 = 1700\ s^{-1}$, $A_1 = 0.20$, $A_2 = 0.80$, where Γ_i is the decay rate and A_i is the amplitude for each mode.

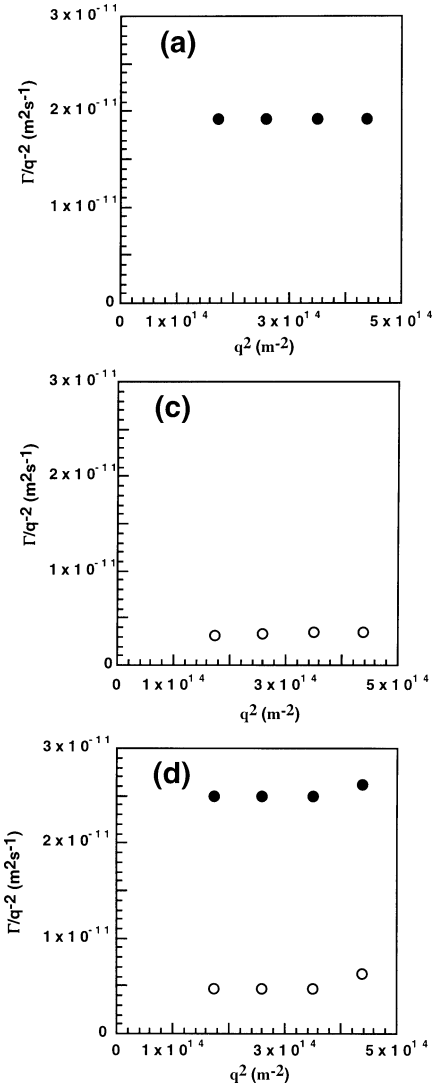

Figure 13. Γ/q^2 vs q^2 plot ((●) fast mode and (○) slow mode) for (a) poly(HOVE-*b*-TFEOVE) (c) poly(HOVE-*b*-HFBOVE), and (d) poly(HOVE)-*b*-NBVE solubilizing DFB.

b-TFEOVE) formed spherical micelles and poly(HOVE-*b*-HFBOVE) formed rodlike micelles reducing the micelle radius, while poly(HOVE-*b*-NBVE) formed both spherical and rodlike micelles also reducing the micelle radius. Solubilization of a hydrophobic compound is usually thought to cause an increase of the micelle size.[30] However, the solubilization significantly reduced the micelle size in our case. The reason for this unusual phenomenon is unknown, but there may be a possibility that the copolymer micelle structure before solubilization was not thermodynamically stable and the solubilization accelerated the transformation to a more stable structure. The polymer micellar system often has very slow dynamics in chain exchange between micelles or micelle-unimer,[31] which may cause fairly long-term structural transformations. Investigation on the time evolution of the micelle structure is now in progress.

Conclusions

Well-defined water-soluble amphiphilic block copolymers bearing three, five, and seven fluorine atoms per monomer unit in the hydrophobic segment were synthesized. These copolymers have very high surface activity so that the surface tension of the aqueous solution is reduced to about 30 mN/m. Direct dissolution of the block copolymer in water above cmc produced copolymer aqueous solutions, where core−shell rodlike and/or core−shell spherical micelles existed. SANS, SAXS, and DLS analyses revealed a trend that a block copolymer bearing larger fluorinated groups was more likely to form rodlike micelles whereas the cross-sectional radii of the micelles was kept rather constant. However, we cannot simply discuss the effect of fluorination of the copolymers on the micellization on this stage, since NBVE has a chemical structure different from TFEOVE, PFPOVE, and HFBOVE (i.e., NBVE have only one ether oxygen atom in one unit, while the others have two oxygen atoms).

We found that the fluorine-containing block copolymer could selectively solubilize fluorinated compounds into water phase, and the fluorinated compounds selectivity was improved with the increase of fluorine atoms per monomer unit, which indicates the "fluorophilicity" of the block copolymer micelles.

Scattering analysis of the copolymer micelle solutions with hydrophobic dyes suggested that the solubilization strongly affected the micelle structures. The fraction of spherical micelles became higher for poly(HOVE-*b*-TFEOVE), while that for poly(HOVE-*b*-HFBOVE) became lower. The cross-sectional radius of micelle became smaller in all samples examined. One can expect that the micelle structures with different solubilizates may not be the same, though the difference between solubilizing fluorinated dye and nonfluorinated dye could not be observed in this study. A control of the micelle

structure by addition of a specific compound is currently under investigation in our laboratory.

Acknowledgment. The present work was supported by a Grant-in-aid for Scientific Research (No. B12555266) and 21st century COE program, COE for a United Approach to New Materials Science from the Ministry of Education, Science, Sports, and Culture of Japan. It was also supported by a Grant-in-aid for Encouragement of Young Scientists (No. 11750764) from the Japan Society for the Promotion of Science. We are deeply grateful to Prof. H. Yamaoka of the University of Shiga Prefecture for useful discussions. We also thank Prof. M. Shibayama and Dr. M. Nagao for their kind support of SANS measurements at Tokai, which was adopted as Proposal 01.08.

References and Notes

(1) Pittman, A. G. In *Fluoropolymers*; Wall, L. A., Ed.; Wiley: New York, 1977.
(2) Sheirs, J., Ed. In *Modern Fluoropolymers*; John Wiley & Sons: New York, 1997.
(3) Kissa, E., Ed. In *Fluorinated Surfactants;* Surfactant Science Series Vol. 50; Marcel Dekker: New York, 1994.
(4) For review of amphiphilic block copolymers, see: Alexandridis, P., Lindman, B., Eds. *Amphiphilic Block Copolymers: Self-Assembly and Applications*; Elsevier: Amsterdam, 2000.
(5) For anionic and group transfer polymerizations, see: (a) Ishizone, T.; Sugiyama, K.; Sakano, Y.; Mori, H.; Hirao, A.; Nakahama, S. *Polym. J.* **1999**, *31*, 983. (b) Krupers, M.; Möller, M. *Macromol. Chem. Phys.* **1997**, *198*, 2163.
(6) For cationic polymerizations, see: (a) Vandooren, C.; Jérôme, R.; Tessié, P. *Polym. Bull. (Berlin)* **1994**, *32*, 387. (b) Höpken, J.; Mëller, M. *Makromol. Chem.* **1992**, *193*, 275.
(7) For radical polymerizations, see: (a) Destarac, M.; Matyjaszewski, K.; Silverman, E.; Ameduri, B.; Boutevin, B. *Macromolecules* **2000**, *33*, 4613. (b) Jol, S.; Lee, W.; Ahn, B.; Park, K.; Kim, K.; Paeng, I. R. *Polym. Bull. (Berlin)* **2000**, *44*, 1. (c) Xia, J.; Johnson, T.; Gaynor, S. G.; Matyjaszewski, K.; DeSimone, J. *Macromolecules* **1999**, *32*, 4802. (d) Zhang, Z.; Ying, S.; Shi, Z. *Polymer* **1999**, *40*, 5439. (e) Zhang, Z.; Ying, S.; Shi, Z. *Polymer* **1999**, *40*, 1341.
(8) Miyamoto, M.; Aoi, K.; Saegusa, T. *Macromolecules* **1989**, *22*, 3540.
(9) (a) Matsumoto, K.; Kubota, M.; Matsuoka, H.; Yamaoka, H. *Macromolecules* **1999**, *32*, 7122. (b) Matsumoto, K.; Mazaki, H.; Nishimura, R.; Matsuoka, H.; Yamaoka, H. *Macromolecules* **2000**, *33*, 8295.
(10) (a) Kamigaito, M.; Sawamoto, M.; Higashimura, T. *Macromolecules* **1992**, *25*, 2587. (b) Sawamoto, M. *Prog. Polym. Sci.* **1991**, *16*, 111.
(11) Aoshima, S.; Nakamura, T.; Uesugi, N.; Sawamoto, M.; Higashimura, T. *Macromolecules* **1985**, *18*, 2097.
(12) Matsumoto, K.; Nishimura, R.; Mazaki, H.; Matsuoka, H.; Yamaoka, H. *J. Polym. Sci., Part A: Polym. Chem.* **2001**, *39*, 3751.
(13) Kamigaito, M.; Maeda, Y.; Sawamoto, M.; Higashimura, T. *Macromolecules* **1993**, *26*, 1643.
(14) Ise, N.; Okubo, T.; Kunugi, S.; Matsuoka, H.; Yamamoto, K.; Ishii, Y. *J. Chem. Phys.* **1984**, *81*, 3294.
(15) Nakano, M.; Matsuoka, H.; Yamaoka, H.; Poppe, A.; Richter, D. *Macromolecules* **1999**, *32*, 697.
(16) In this polymer system, the hydrophobicity of the core-forming segment is sufficiently high that the micelle core should be composed only of the hydrophobic polymer. Indeed, calculations using models with a water-containing core gave less fitted curves than those calculated without considering the water in the core.
(17) Richter, D.; Schneider, D.; Monkenbusch, M.; Willner, L.; Fetters, L. J.; Huang, J. S.; Lin, M.; Mortensen, K.; Farago, B. *Macromolecules* **1997**, *30*, 1053.
(18) Matsuoka, H.; Yamamoto, Y.; Nakano, M.; Endo, H.; Yamaoka, H.; Zorn, R.; Monkenbusch, M.; Richter, D.; Seto, H.; Kawabata, Y.; Nagao, M. *Langmuir* **2000**, *16*, 9177.
(19) Pedersen, J. S.; Gerstenberg, M. C. *Colloids Surf., A* **2003**, *212*, 175.
(20) Nakano, M.; Deguchi, M.; Matsumoto, K.; Matsuoka, H.; Yamaoka, H. *Macromolecules* **1999**, *32*, 7437.
(21) Mortensen, K.; Brown, W.; Almdal, K.; Alami, E.; Jada, A. *Langmuir* **1997**, *13*, 3635.
(22) Jada, A.; Hurtrez, G.; Siffert, B.; Riess, G. *Macromol. Chem. Phys.* **1996**, *197*, 3697.
(23) Glatter, O.; Scherf, G.; Schillen, K.; Brown, W. *Macromolecules* **1994**, *27*, 6046.
(24) Mortensen, K.; Pedersen, J. S. *Macromolecules* **1993**, *26*, 805.
(25) Wu, G.; Chu, B.; Schneider, D. K. *J. Phys. Chem.* **1995**, *99*, 5094.
(26) Israelachivili, J. *Intermolecular & Surface Forces*; Academic: New York, 1992; Chapter 17.
(27) (a) Corkill, J. M.; Goodman, J. F.; Harrold, S. P. *Trans. Faraday Soc.* **1964**, *60*, 202. (b) Corkill, J. M.; Goodman, J. F.; Ottewill, R. H. *Trans. Faraday Soc.* **1961**, *57*, 1627.
(28) (a) Zielinski, R.; Ikeda, S.; Nomura, H.; Kato, S. *J. Colloid Interface Sci.* **1989**, *129*, 175. (b) Hayashi, S.; Ikeda, S. *J. Phys. Chem.* **1980**, *84*, 744. (c) Ikeda, S.; Ozeki, S.; Tsunoda, M. *J. Colloid Interface Sci.* **1980**, *73*, 27. (d) Kushner, L. M.; Hubbard, W. D.; Parker, R. *J. Res. Natl. Bur. Stand.* **1957**, *59*, 113. (e) Ozeki, S.; Ikeda, S. *Colloid Polym. Sci.* **1984**, *262*, 409. (f) Imae, T.; Ikeda, S. *Colloid Polym. Sci.* **1987**, *265*, 1090. (g) Ikeda, S. *Colloid Polym. Sci.* **1991**, *268*, 49. (h) Ozeki, S.; Ikeda, S. *J. Colloid Interface Sci.* **1982**, *97*, 424.
(29) Maeda, S.; Matsumoto, K.; Matsuoka, H. *Polym. Prepr. Jpn.* **2002**, *51*, 2350.
(30) (a) Hurter, P. N.; Scheutjiens, J. M. H. M.; Hatton, T. A. *Macromolecules* **1993**, *26*, 5030. (b) Hurter, P. N.; Scheutjiens, J. M. H. M.; Hatton, T. A. *Macromolecules* **1993**, *26*, 5592.
(31) For examples see: (a) Iyama, K.; Nose, T. *Macromolecules* **1998**, *31*, 7356. (b) Creutz, S.; Stam, J.; De Schryver, F. C.; Jérôme, R. *Macromolecules* **1998**, *31*, 681. (c) Esselink, F. J.; Dormidontova, E.; Hadziioannou, G. *Macromolecules* **1998**, *31*, 2925. (d) Smith, C. K.; Liu, G. *Macromolecules* **1996**, *29*, 2060. (e) Malmsten, M.; Lindman, B. *Macromolecules* **1992**, *25*, 5440.

MA021166I